Weakly nonparaxial effects on the propagation of (1+1)D spatial solitons in inhomogeneous Kerr media

A. Suryanto[1,*], **E. van Groesen**[2] **and M. Hammer**[2]
[1]Applied Mathematical Modeling and Computation Laboratory,
Jurusan Matematika, Universitas Brawijaya, Indonesia
[2] Applied Analysis and Mathematical Physics,
MESA+ Research Institute, University of Twente, The Netherlands

Abstract

The widely used approach to study the beam propagation in Kerr media is based on the slowly varying envelope approximation (SVEA) which is also known as the paraxial approximation. Within this approximation, the beam evolution is described by the nonlinear Schrödinger (NLS) equation. In this paper, we extend the NLS equation by including higher order terms to study the effects of nonparaxiality on the soliton propagation in inhomogeneous Kerr media. The result is still a one-way wave equation which means that all back-reflections are neglected. The accuracy of this approximation exceeds the standard SVEA. By performing several numerical simulations, we show that the NLS equation produces reasonably good predictions for relatively small degrees of nonparaxiality, as expected. However, in the regions where the envelope beam is changing rapidly as in the break up of a multisoliton bound state, the nonparaxiality plays an important role.

Keywords: Nonparaxiality, inhomogeneous Kerr medium, multisoliton bound state (higher-order soliton)

1 Introduction

The study of nonlinear effects on the propagation of electromagnetic waves has been of considerable recent interest. One of the widely studied nonlinear optical phenomena is the self-focusing of light beams in a nonlinear Kerr medium; see e.g., [1]-[2]. In a Kerr medium, which possesses a positive intensity-dependent change of refractive index, a high power light beam may focus by creating a lenslike index profile for itself. When it is balanced by diffraction, the self-focusing can lead to the formation of a self-trapped light beam. In $(1+1)$D, as in a planar waveguide,

*Address: Jurusan Matematika, Universitas Brawijaya, Jl. Veteran Malang 65145, Indonesia; E-mail : suryanto@brawijaya.ac.id

this kind of balancing is stable against all perturbations as shown by Zakharov and Shabat [3], and therefore forms a genuine spatial soliton. Here $(m+1)$D is meant for m transverse dimensions and one propagation direction. Spatial solitons have attracted great interest due to the fascinating phenomena encountered and their potential applications to all-optical data processing devices; see e.g., [1], [2] and [4].

In the widely used approach, the analysis of light beams propagating in Kerr media is based on the nonlinear Schrödinger (NLS) equation. In deriving the NLS equation, one makes the slowly varying envelope approximation (SVEA) in the propagation direction (or paraxial approximation). In this paper we will study the effects of nonparaxiality in order to investigate the validity of the $(1+1)$D NLS equation. This is motivated by the appearance of large variations in amplitude that may result from the bi-plane wave deformation (i.e. the spatial analog of a bichromatic pulse in uniform medium [5]), or from the splitting process of the break up of multisoliton bound states, see e.g., [6], [7] and [8].

The validity of the SVEA is, in fact, already questioned for a long time. It was started by the prediction of [9] in 1965 that the $(2+1)$D NLS equation may produce a catastrophic collapse of a self-focusing beam, i.e. the beam amplitude blows up to infinity. With the probability for a collapse, a considerable part of studies on the self-focusing phenomenon has been directed towards finding mechanisms that arrest the collapse. It has been shown that a medium with saturable nonlinearity (see e.g. [10] and [11]) and negative contributions to the index of refraction due to avalanche ionization [12] as well as a quintic nonlinearity [13] can arrest the collapse. However, these are properties specifying the given medium, while, as pointed out by Feit and Fleck [14], the self-focusing occurs in a variety of media without catastrophic collapse. This justifies the necessity of a medium-independent mechanism model which yields beams with nonsingular behavior. In this direction, Feit and Fleck [14] showed that the unphysical collapse is due to the invalidity of the paraxial wave equation during the advanced stages of self-focusing. They showed that if the nonparaxiality is included then the self-focusing is noncatastrophic, i.e. the nonparaxiality replaces the catastrophic focusing with a sequence of focusing-defocusing cycles. This behavior is confirmed both numerically by Akhmediev *et al.* ([15] and [16]), by Sheppard and Haelterman [17] and analytically by Fibich [18].

Up to now, most works on the effects of the nonparaxiality have been restricted to study the phenomenon of the catastrophic self-focusing arrest. Different from the $(2+1)$D case, based on the inverse scattering method, an optical beam propagating in $(1+1)$D is predicted to be stable against collapse. Therefore the effects of the nonparaxiality in $(1+1)$D received only little attention. Here we will study the effects of the nonparaxiality on $(1+1)$D beam propagation in Kerr media. To do so, we derive a beam propagation model which includes the weak nonparaxiality using perturbation theory in section 2. In section 3 we derive a conserved quantity of the present model and compare with those of the nonlinear Helmholtz (NLH) and NLS equations. The soliton propagation in uniform media and in a Gaussian waveguide are respectively discussed in section 4 and section 5. In section 6 we study the break up of a two-soliton bound state in a Gaussian waveguide. Finally, conclusions and remarks are given in the last section.

2 Nonparaxial correction to the NLS equation

We study the propagation of light along the z axis of a planar Kerr waveguide. As shown in [8], in the presence of a transverse linear refractive index variation, the evolution of the evelope of the nonparaxial beam is described by the following NLH equation:

$$i\frac{\partial B}{\partial Z}+\frac{1}{2}\frac{\partial^2 B}{\partial X^2}+|B|^2 B+\Delta n B+\kappa^2\left(\frac{1}{2}\frac{\partial^2 B}{\partial Z^2}+\frac{1}{2}\ \Delta n^2 B\right)=0, \tag{1}$$

where the scaled transverse index variation $\Delta n \equiv \Delta n\,(X)$ is small, i.e. of the order κ. In Equation (1), X, Z and B are dimensionless variables where their corresponding physical quantities are determined by the following transformation

$$\begin{aligned} x &= \frac{X}{\kappa k_0}, \\ z &= \frac{Z}{\kappa^2 k_0}, \\ A\,(x,z) &= \kappa\sqrt{n_0/n_2}B\,(X,Z)\,. \end{aligned} \tag{2}$$

Here n_0 is the linear refractive index constant, $k_0 = \omega n_0/c$ is the wavenumber of the carrier wave and n_2 is the coefficient of the nonlinear refractive index. The small nonparaxiality parameter $0 < \kappa \ll 1$ can be related to the ratio of the input vacuum wavelength λ_0 and the input beam width $w_0 : \kappa = \lambda_0/\left(2\pi w_0\right)$. The relation between the beam envelope $A\,(x,z)$ and the electric field is given by

$$\mathbf{E}=\frac{1}{2}\left\{A\,(z,x)\exp\left[i\left(k_0 z-\omega t\right)\right]+cc.\right\}\cdot\mathbf{y}. \tag{3}$$

Equation (1) is an elliptic equation. In order to solve the NLH equation numerically, we have to provide boundary conditions that limit the computational domain. In our case, the required boundary conditions have to be transparent for all outgoing waves and simultaneously model the incident waves; such conditions are called Transparent-Influx Boundary Conditions (TIBC). To the best of our knowledge, a proper TIBC for inhomogeneous nonlinear media is not known. Furthermore, apart from the lack of TIBC, to perform accurate numerical simulations we usually need a very large number of grid points, making the computations too expensive for a standard personal computer. Therefore, the standard approach in solving the NLH equation numerically is to approximate it with an initial value problem. The simplest approximation of Equation (1) that is correct up to $\mathcal{O}\left(\kappa^2\right)$ takes the form of the inhomogeneous NLS equation:

$$i\frac{\partial B}{\partial Z}+\frac{1}{2}\frac{\partial^2 B}{\partial X^2}+|B|^2 B+\Delta n B=0. \tag{4}$$

Equation (4) is derived from Equation (1) by neglecting the nonparaxial effects (the first term in brackets) and high order terms. In fact, the size of the nonparaxial effect which arises from the non-slowly varying envelope (non-SVE) is determined by the value of κ^2. If κ^2 is large enough then the nonparaxial effect may become important and therefore it can no longer be neglected. To reveal the effect of nonparaxiality we will improve the NLS equation (4) by including terms of the order up to κ^3. To this end, we will evaluate the non-SVE term in the NLH equation by noting that

$$\frac{\partial B}{\partial Z} = i\left(\frac{1}{2}\frac{\partial^2 B}{\partial X^2} + |B|^2 B + \Delta n B\right) \tag{5}$$

is accurate up to order κ where the contribution of the order of κ^2 and smaller have been neglected. Then the non-SVE contribution can be approximated in order κ^3 :

$$\begin{aligned}
\frac{\kappa^2}{2}\frac{\partial^2 B}{\partial Z^2} \approx \frac{\kappa^2}{2} i &\left[\frac{1}{2}\frac{\partial^3 B}{\partial Z \partial X^2} + \Delta n \frac{\partial B}{\partial Z} + \frac{\partial\left(|B|^2 B\right)}{\partial Z}\right] \\
= -\frac{\kappa^2}{2} &\left[\frac{1}{4}\frac{\partial^4 B}{\partial X^4} + \left(\frac{1}{2}\frac{\mathrm{d}^2\Delta n}{\mathrm{d}X^2} + \Delta n^2\right) B + \frac{\mathrm{d}\Delta n}{\mathrm{d}X}\frac{\partial B}{\partial X}\right. \\
&+ \left(\Delta n + |B|^2\right)\frac{\partial^2 B}{\partial X^2} + 2\Delta n |B|^2 B + |B|^4 B \\
&\left. + \frac{1}{2}\frac{\partial^2\left(|B|^2 B\right)}{\partial X^2} - \frac{1}{2}B^2\frac{\partial^2 B^*}{\partial X^2}\right],
\end{aligned} \tag{6}$$

where B^* stands for the complex conjugate of B. The approximation in (6) represents one step beyond the slowly varying envelope approximation (SVEA) applied in the NLS equation, but still assumes a slowly varying envelope such that further nonparaxial terms of the order κ^4 and higher order terms can be neglected. In other words, the nonparaxial effect is assumed to be weak but nonvanishing.

By replacing the nonparaxial term in Equation (1) with its approximation (6), we obtain a higher-order nonlinear beam propagation equation

$$\begin{aligned}
i\frac{\partial B}{\partial Z} + \frac{1}{2}\frac{\partial^2 B}{\partial X^2} + |B|^2 B + \Delta n B = \frac{\kappa^2}{2} &\left[\frac{1}{4}\frac{\partial^4 B}{\partial X^4} + \frac{1}{2}\frac{\mathrm{d}^2\Delta n}{\mathrm{d}X^2} B + \frac{\mathrm{d}\Delta n}{\mathrm{d}X}\frac{\partial B}{\partial X}\right. \\
&+ 2\Delta n |B|^2 B + \left(\Delta n + |B|^2\right)\frac{\partial^2 B}{\partial X^2} + |B|^4 B \\
&\left. + \frac{1}{2}\frac{\partial^2\left(|B|^2 B\right)}{\partial X^2} - \frac{1}{2}B^2\frac{\partial^2 B^*}{\partial X^2}\right].
\end{aligned} \tag{7}$$

From now on we call this equation the nonparaxial nonlinear Schrödinger (NNLS) equation. Further improvement could be done iteratively but will not be treated here. Equation (7) takes the form of our standard inhomogeneous NLS equation (4) with perturbations which arise from the nonparaxiality. The perturbations include the linear nonparaxial diffraction, linear refractive index change, the diffraction that depends on the transverse index variation and on the intensity and the quintic nonlinearity. We remark that although Equation (7) involves higher-order contributions, it still neglects the coupling between forward-propagating waves and backscattering.

However, with this approximation, the problem is greatly simplified when it is solved numerically. Indeed the resulting equation is still a one-way wave equation. The numerical study of a beam propagating in both homogeneous and inhomogeneous media with Kerr nonlinearity under the influence of weak nonparaxiality will be given in the next sections. For this purpose the NNLS equation (7) is solved numerically using an implicit Crank-Nicolson scheme [19] and transparent boundary conditions [20].

Remark *In the normalized (inhomogeneous) NLS equation (4), the parameter* κ *does not appear explicitly. Therefore the simulation results of this equation can be interpreted for any* κ*. As an example, for given two different values of* κ*, say* κ_0 *and* κ_1*, the normalized NLS equation for those* κ*'s with the same normalized initial conditions will produce exactly the same results. However, according to Equation (2), the real physical situations are different. To distinguish between the results of paraxial and nonparaxial approaches, the results of paraxial approximation (NLS equation) are denoted by* $\kappa = 0$*.*

3 Power conservation law

Before proceeding the numerical study, we will investigate the power flow conservations of the NLH equation and its approximations. To that end, we multiply Equation (1), (4) and (7) respectively by B^*, subtract the complex conjugate of it, and then integrate the resulting expression over the whole transverse coordinate. With this procedure we obtain the power flow invariant for the NLH equation

$$\frac{\mathrm{d}}{\mathrm{d}Z}\left[P_{\mathrm{NLH}}\right] = 0, \tag{8}$$

which means that the value of

$$P_{\mathrm{NLH}} = \int_{-\infty}^{\infty} \left[|B|^2 - i\frac{\kappa^2}{2}\left(B^* \frac{\partial B}{\partial Z} - B\frac{\partial B^*}{\partial Z} \right) \right] \,\mathrm{d}X \tag{9}$$

is a conserved quantity during propagation. P_{NLH} represents the dimensionless component of the Poynting vector $\mathbf{S} = \frac{1}{2}\mathrm{Re}\left\{\mathbf{E}\times\mathbf{H}^*\right\}$ in the propagation direction integrated over the whole transverse coordinate. This result is expected physically because in general theory of wave propagation in media without loss or gain, the power flow is a quantity that has to be constant. However, in the NLS equation, this conservation law is incomplete as the nonparaxial effect is completely neglected, i.e. only the first term in Equation (9):

$$P_{\mathrm{NLS}} = \int_{-\infty}^{\infty} |B|^2 \,\mathrm{d}X \tag{10}$$

is conserved. In the case of weak nonparaxiality such that the beam evolution takes the form of the NNLS equation (7), we obtain the approximate power conservation law in the form

$$P_{\mathrm{NNLS}} = \int_{-\infty}^{\infty} \left[|B|^2 + \frac{\kappa^2}{2} |B|^4 \right] \, \mathrm{d}X + \mathcal{O}\left(\kappa^4\right), \tag{11}$$

which means that for the same initial input, $P_{\mathrm{NNLS}} \geq P_{\mathrm{NLS}}$. We note that Equation (11) can also be derived by directly substituting Equation (5) into Equation (9). We further notice that P_{NLH} and P_{NNLS} differ only by $\mathcal{O}\left(\kappa^4\right)$ while the difference between P_{NLH} and P_{NLS} is $\mathcal{O}\left(\kappa^2\right)$. The conservation laws (9) and (11) reduce to the paraxial conservation law (10) only if $\kappa^2 \longrightarrow 0$.

4 Soliton propagation in uniform media

Before studying the propagation of a soliton in inhomogeneous media, we consider first the case of a uniform medium, i.e. the index variation $\Delta n = 0$. For this case, we look for a stationary soliton solution of these three equations (NLH, NLS, NNLS) by assuming that a shape-preserving solution exists and has the form

$$B(X, Z) = f(X) \exp(i\beta Z), \tag{12}$$

where both f and df/dX vanish as $|X| \to \infty$. Then we substitute this Ansatz into the three equations, respectively, and solve the resulting equations for f and β by assuming that $f = \eta$ and $df/dX = 0$ at the soliton peak (which is assumed to occur at $X = 0$). We find that the three model equations (NLH, NLS, NNLS) have an exact soliton solution with the same profile but with different longitudinal wavenumbers β :

$$B(X, Z) = \eta \operatorname{sech}(\eta X) \exp(i\beta Z). \tag{13}$$

The longitudinal wavenumber of the NLH soliton is determined by the quadratic equation: $(1/2)\,\kappa^2 \beta_{\mathrm{NLH}}^2 + \beta_{\mathrm{NLH}} - (1/2)\,\eta^2 = 0$, i.e.

$$\beta_{\mathrm{NLH}} = \left(-1 + \sqrt{1 + \kappa^2 \eta^2}\right) / \kappa^2. \tag{14}$$

The positive sign in front of the square root in Equation (14) is chosen in order to be consistent with the wavenumbers of the NLS and NNLS solitons which are respectively given by

$$\beta_{\mathrm{NLS}} = \frac{1}{2}\eta^2, \tag{15}$$

$$\beta_{\mathrm{NNLS}} = \left(\frac{1}{2}\eta^2 - \frac{1}{8}\kappa^2 \eta^4\right). \tag{16}$$

To see the relation between the solution of the NLH equation and its approximations, we write the Taylor expansion of β_{NLH} by assuming that $\kappa^2 \eta^2$ is small:

$$\beta_{\mathrm{NLH}} \approx \frac{1}{2}\eta^2 - \frac{1}{8}\kappa^2 \eta^4 + \mathcal{O}\left(\kappa^4\right). \tag{17}$$

It is evident that the wavenumbers of the stationary solution of both NLS and NNLS equations are approximations of β_{NLH} but with different order of accuracy. This fact supports the conclusion that the NNLS equation is the reduction of the NLH equation which includes the lowest order nonparaxial correction under the NLS scaling. We remark that in the case of the exact stationary solution, the value of P_{NLS} is also a conserved quantity of the NNLS equation. This can be checked from the fact that the profile of the stationary solution of the NNLS equation is not deformed during propagation. Now we study the effect of nonparaxiality in the case where the initial profile will distort during the evolution, i.e. by considering the initial value problem (IVP) through Equation (7) with an initial condition:

$$B\left(X,0\right) = \eta^{\pm}\mathrm{sech}\left(X\right), \tag{18}$$

where $\eta^{\pm} = 1 \pm 0.1$. Notice that the initial condition (18) corresponds to a stationary soliton but with a perturbed-amplitude. In the regime of the paraxial approximation, it is well known from the inverse scattering method that the initial condition with (18) produces a soliton of unit amplitude plus radiation; see e.g. [21] and [22]. However, to the best of our knowledge, there is no exact theory that describes this IVP that includes the nonparaxiality. Therefore we will study this IVP numerically by solving Equation (7) with initial data (18).

In Figure 1 we compare the numerical results of the NLS and the NNLS equations for amplitude η^{+} and $\kappa^2 = 0.01$. We observe that in both paraxial and nonparaxial models, a "soliton" with a small excess amplitude (η^{+}) initially experiences self-focusing (the amplitude increases in the middle and the beam width becomes narrower). When it reaches the maximum amplitude, the soliton starts to defocus and emits radiation. The focusing-defocusing behavior with releasing radiation is repeated almost periodically. The direct observation of the amplitude during propagation shows that the quantitative difference between the paraxial and nonparaxial models is very small, see Figure 1.(a) and (b). However, a closer look indicates that the nonparaxiality produces a longer period of the focusing-defocusing cycles (see Figure 1.(b)). Furthermore, by monitoring the energy conservation, we conclude that the paraxial and nonparaxial beam propagation include different physical mechanisms. Indeed, in the case of the NLS equation although the beam follows a series of decaying focusing-defocusing oscillations which resembles the effect of diffraction and Kerr nonlinearity, P_{NLS} remains constant, see Figure 1. However, when the nonparaxiality is included in the calculation, the value of P_{NLS} is oscillating while P_{NNLS} is conserved. Figure 1.(b) and 1.(c) shows that when the beam is narrowing the contribution of the nonparaxial term in P_{NNLS} increases, taking the energy from the paraxial part which therefore decreases the NLS invariant P_{NLS}. When the beam becomes wider (diffracts), our numerical results show that P_{NLS} increases, as expected.

When the initial "soliton" has a small deficit amplitude (η^{-}), our numerical calculations based on the paraxial and nonparaxial equations also show that the beam experiences a defocusing-focusing oscillation rather than directly diffracts into radiation, see Figure 2. Diffraction broadening for both paraxial and nonparaxial cases

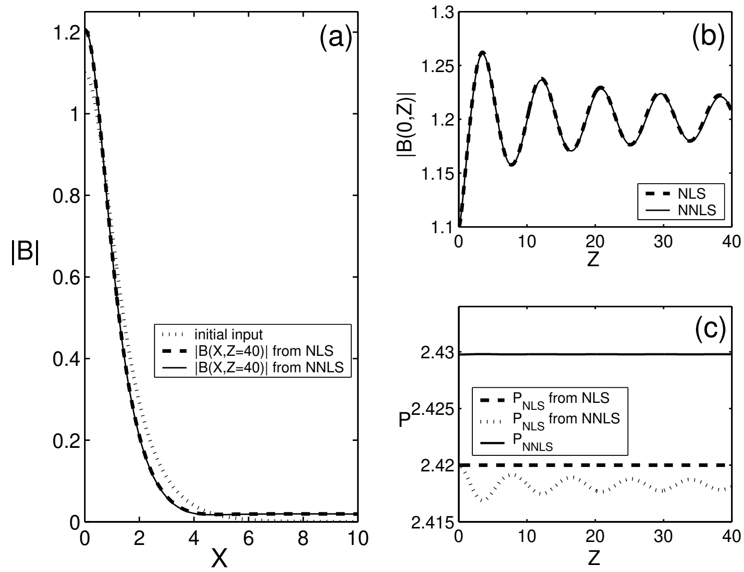

Figure 1: Propagation of a soliton with amplitude 10% higher ($\eta^+ = 1.1$) for $\kappa^2 = 0.01$ over a distance $Z = 40$. (a) The beam profiles at the final position obtained from the NLS equation (dashed) and from the NNLS equation (solid). For comparison, the initial profile is also plotted (dotted). (b) Evolution of the on-axis amplitude $|B(0,Z)|$ showing that both paraxial and nonparaxial beams exhibit decaying focusing-defocusing cycles. (c) Evolution of P_{NLS} and P_{NNLS}. When the beam focuses (defocuses) the energy P_{NLS} obtained from then NNLS equation (dotted) decreases (increases) while that calculated from the NLS equation (dashed) is conserved. The conserved energy of the NNLS (P_{NNLS}) is also plotted (solid).

occurs only when the "soliton" amplitude is much smaller than 1. The defocusing-focusing behavior of the paraxial "soliton" is expected because the stationary paraxial soliton in (1+1)D is stable against a small change of initial data. This is different from the case of the paraxial soliton in (2+1)D where the soliton beam with initial energy deficit will experience diffraction broadening. Under the nonparaxial effect, for a small excess or a deficit amplitude, P_{NLS} shows an oscillatory behavior; showing that the nonparaxial contributions control the mechanism of self-focusing and defocusing (due to diffraction). In (1+1)D case, this behavior may be considered to be less important. However, this phenomenon becomes essential in (2+1)D in order to stabilize the soliton beam [17].

5 Soliton propagation in non-uniform media

The propagation of a single soliton beam in an inhomogeneous medium under the paraxial approximation which is modeled by Equation (4) has been studied. As an example, when the inhomogeneity $\Delta n\,(X)$ has a triangular profile, called a triangular waveguide, it has been shown that a stationary soliton beam placed in one side of a

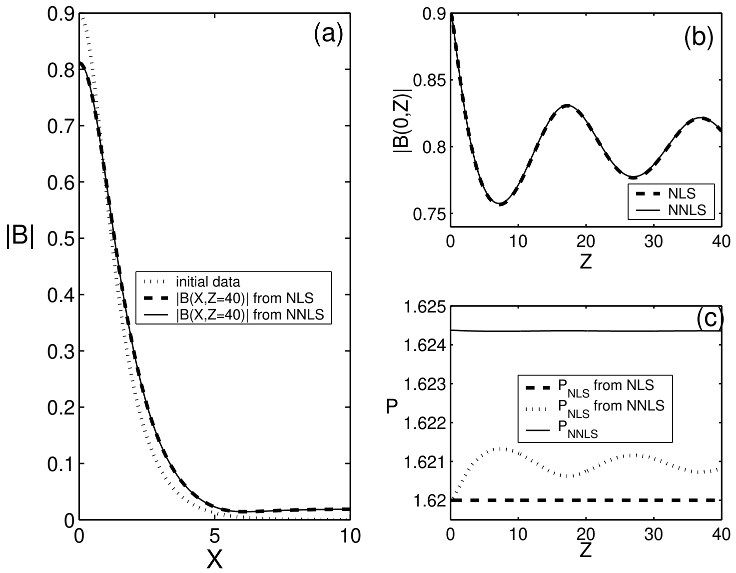

Figure 2: Same as for Figure 1, but for deficit amplitude $\eta^{-} = 0.9$. The amplitude oscillation shows the soliton stability.

triangular waveguide will oscillate periodically around the center of the waveguide [6]. A similar soliton behavior has been observed when $\Delta n\,(X)$ has a Gaussian profile [23]. In this section we study the effects of nonparaxiality on this behavior. As discussed in section 2, the governing equation that includes the nonparaxial contributions takes the form of the NNLS equation (7). To avoid the singularity of the derivative of the transverse index variation which may cause a numerical problem, we assume that Δn has a Gaussian profile:

$$\Delta n\,(X) = \Delta n_0 \exp\left(-bX^2\right) \tag{19}$$

rather than a triangular profile. Here, Δn_0 is the maximum index variation and b is a constant that controls the width of the waveguide. To see the effect of nonparaxiality, we first look back to the stationary soliton solution of the homogeneous NLS and NNLS equations, see Equation (13), where the longitudinal wavenumbers are respectively given by Equation (15) and Equation (16). It is clear that for $\kappa \neq 0$ the longitudinal wavenumber of the nonparaxial soliton is always smaller than that of the paraxial soliton of the same amplitude. We note that $\kappa = 0$ means the beam has infinite width. Indeed, the difference between β_{NLS} and β_{NNLS} is

$$\beta_{NLS} - \beta_{NNLS} = \kappa^2\eta^4/8. \tag{20}$$

As a result the longitudinal wavelength of the nonparaxial soliton is larger than that of the paraxial one. That is to say, the nonparaxial soliton experiences a larger longitudinal force (F_Z). Now we make an assumption (that will be justified later), that if a transverse inhomogeneity Δn is introduced then both paraxial and nonparaxial solitons will experience the same transversal force (F_X) at any X which in combination with the longitudinal force F_Z causes an oscillatory behavior as mentioned above. Since the nonparaxial soliton experiences a larger F_Z than the paraxial one, it will have a longer oscillation period. This situation is illustrated schematically in Figure 3. From Equation (20) we conclude that the difference between the oscillation period of the nonparaxial and that of the paraxial case is larger for a larger degree of nonparaxiality κ or for a higher soliton amplitude η.

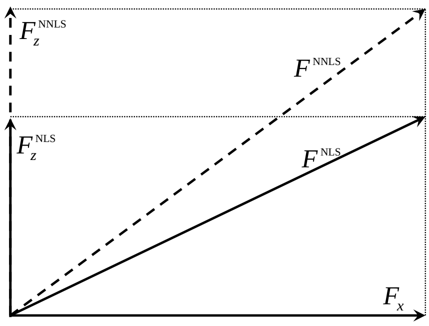

Figure 3: In the mechanical analogy, both paraxial and nonparaxial solitons in a Gaussian waveguide experience the same transversal force (F_x) but different longitudinal forces (F_z). Since the longitudinal force in the nonparaxial case is larger, the oscillation period is longer in that case.

To confirm these theoretical predictions, we perform numerical simulations based on Equation (7) using the initial condition

$$B\left(X,0\right)=\eta\mathrm{sech}\left[\eta\left(X-X_0\right)\right], \tag{21}$$

where X_0 represents the initial position of the soliton. In all calculations presented in this section, we take $X_0 = -3.5$, $\Delta n_0 = 0.1$ and $b = 0.1$. In Figure 4 we show the simulation results for $\kappa^2 = 0.001$ and $\kappa^2 = 0.01$ with the same amplitude $\eta = 1$. For comparison we also plot the result of the NLS equation ($\kappa = 0$). Figure 4.(a) shows the oscillatory behavior of the position of the maximum amplitude. It is found that the (normalized) oscillation period for larger κ^2 is longer than that for smaller one. This behavior cannot be seen clearly on the scale of Figure 4.(a) because the differences between the oscillation period of $\kappa^2 = 0.001$ and 0.01 are very small. To see this behavior more clearly we plot in Figure 4.(b) the soliton profiles for different κ^2 at the final position of our simulation, i.e. at $Z = 200$. It is shown here that the soliton for $\kappa^2 = 0.01$ arrives later than the others (remember that Figure 4.(b) corresponds to the left-going beam). The effect of nonparaxiality is more pronounced when we increase the soliton amplitude as one should expect, e.g. see Figure 5 for $\eta = 2$.

To verify that the larger oscillation period caused by the nonparaxial effect is mainly due to the smaller longitudinal wavenumber β, we need to improve the NLS equation (4) in such a way that the homogeneous version of the resulting equation (i.e. for $\Delta n = 0$), called the improved-NLS (iNLS) equation, has a stationary soliton solution with $\beta = \beta_{\rm NNLS}$. One can check that this requirement is satisfied by the following equation

$$i\left(1+\frac{\kappa^2\eta^2}{4-\kappa^2\eta^2}\right)\frac{\partial B}{\partial Z}+\frac{1}{2}\frac{\partial^2 B}{\partial X^2}+\left|B\right|^2B+\Delta nB=0. \tag{22}$$

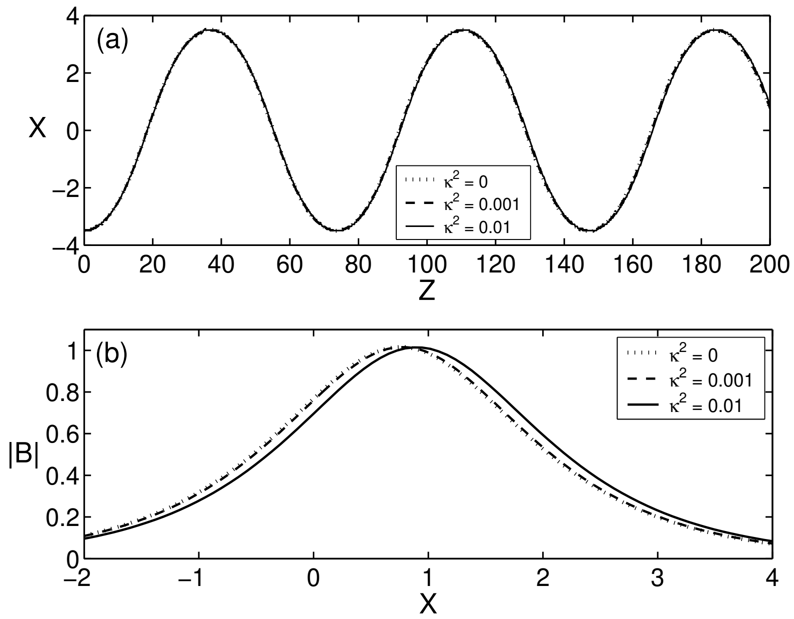

Figure 4: Propagation of a single soliton of amplitude $\eta = 1$ in a Gaussian waveguide for $\kappa^2 = 0, 0.001$ and 0.01. (a) The position of the maximum amplitude, showing the oscillatory behavior of both paraxial and nonparaxial solitons. The differences between the oscillation periods of $\kappa^2 = 0, 0.001$ and 0.01 are very small such that they cannot be seen on the scale of this plot. (b) The period differences are clearly seen in the plot of the soliton profile at the final propagation distance $Z = 200$.

Figure 6 shows the numerical results of Equation (22) for $\eta = 1$ and $\eta = 2$ using $\kappa^2 = 0.01$. It is evident that those results agree quite well to the results of the NNLS equation (7), showing that the iNLS equation indeed improves significantly the period of the soliton oscillation. We conclude that the nonparaxiality in a Kerr medium which has a Gaussian refractive index profile increases the oscillation period.

6 Propagation of multisoliton bound states

We now consider the initial data:

$$B(X, 0) = 2\eta_0 \mathrm{sech}\left[\eta_0 (X - X_0)\right]. \tag{23}$$

The initial data (23), in a uniform medium under the paraxial approximation, generates two single solitons of amplitude $\eta_1 = \eta_0$ and $\eta_2 = 3\eta_0$, respectively [21] and [22]. These two solitons have the same longitudinal velocity and travel together; and therefore this is called a two-soliton bound state or second-order soliton. During the propagation this bound state shows a periodic focusing-defocusing (breathing behavior) without releasing radiation, see e.g. Figure 7.(a). However, if we introduce nonparaxiality, we predict the following phenomena:

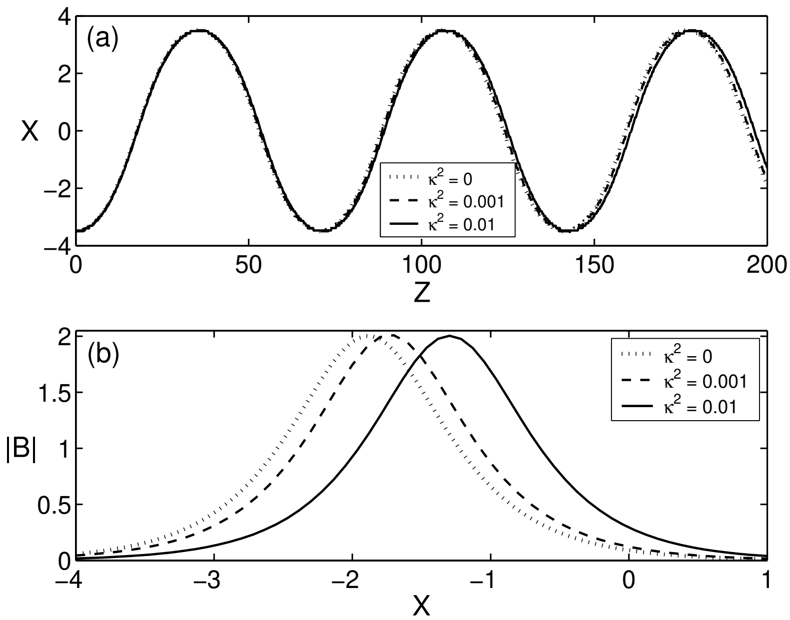

Figure 5: Same as for Figure 4, but for $\eta = 2$. The effect of nonparaxiality is more pronounced compared to that of $\eta = 1$.

- Similar to the case that is presented in section 4, the initial field (23) gives rise to a breathing behavior (periodic focusing-defocusing). However, because this initial condition may be not the perfect initial data to generate a nonparaxial two-soliton bound state, we may expect that the focusing-defocusing cycles are accompanied by radiation.
- By considering that the initial data produces at least one nonparaxial soliton (and the remainder can form another soliton or a radiating entity), these two entities (soliton and the remainder) will have a smaller longitudinal wavenumber compared to their paraxial version. Therefore the period of the focusing-defocusing cycle in the nonparaxial case is larger than that in paraxial one.
- As discussed earlier, the nonparaxiality influences the mechanism of the focusing-defocusing series which in the (2+1)D case can prevent the collapse. This phenomenon can also cause the peak amplitude due to self-focusing in nonparaxial case to be smaller than in paraxial one.

Indeed, those phenomena are confirmed by our numerical simulations. For example we plot the numerical results for the case of $\eta_0 = 1$ and $X_0 = 0$ in Figure 7.

Now we introduce a linear transverse index variation $\Delta n\,(X)$ of the form (19). Under the paraxial approach, the second-order soliton produced by initial data (23) is splitted into two individual solitons since each single soliton, which is hidden in the bound state and initially has the same velocity, experiences a different transverse acceleration. A higher amplitude soliton experiences a larger transverse acceleration.

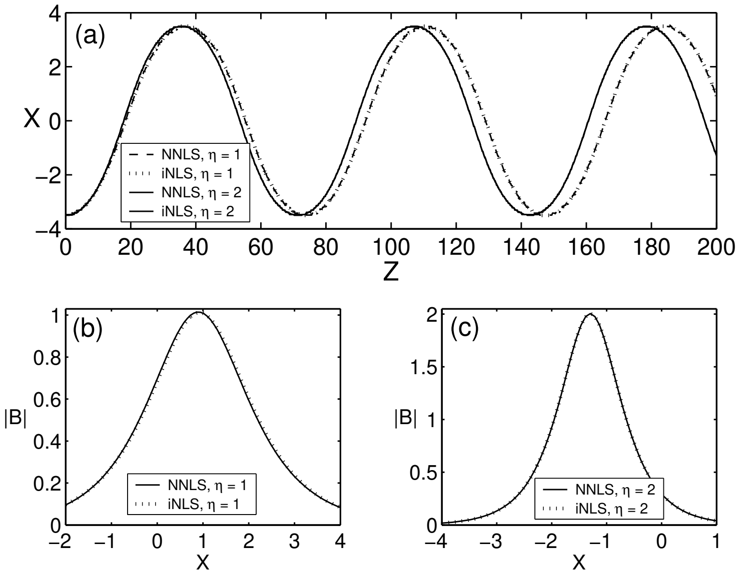

Figure 6: Same as for Figure 4 and 5 but calculated from the iNLS equation for respectively $\eta = 1$ (dotted-line in (a)) and $\eta = 2$ (thin-solid-line in (a)) with $\kappa^2 = 0.01$. Comparison to the results of the NNLS equation shows that the iNLS improves significantly the NLS equation.

The final result of the splitting process, i.e. a soliton either exits or still oscillates and collides with others inside the waveguide, depends on the initial amplitude η_0 [8]. When the nonparaxial effect is taken into account, the oscillation period of the single soliton becomes longer. Since the period extension of the soliton with the larger amplitude is much larger than the one with the smaller amplitude, the nonparaxiality will of course change the splitting process which may cause a very different result. In Figure 8 and 9 we present simulation results of Equation (7) using initial data (23) for two different η_0's and $\kappa^2 = 0.001, 0.01$. In these calculations, the Gaussian waveguide is characterized by $\Delta n_0 = 0.1$ and $b = 0.1$ while the initial position of the bound state is taken to be $X_0 = -3.5$. In nonparaxial simulations, we observe that the field is radiating. However, the radiation is relatively small compared to the amplitude of the core parts. For simplicity, we call the core parts as two solitons with different amplitude (although one or none of them may be just a radiating entity).

In Figure 8, we show the numerical results for $\eta_0 = 0.75$. From the NLS simulation (see Figure 8.(a)), it is shown that the two-soliton bound state is splitted into two individual solitons after some propagation distance where the smaller soliton is expelled to the right of the waveguide while the higher one is oscillating inside the waveguide. The result of the nonparaxial model using $\kappa^2 = 0.001$ also shows a similar behavior: the smaller soliton exits the waveguide after the splitting process, but it is slightly less displaced than the paraxial one with respect to the propagation axis. When we increase the degree of the nonparaxiality to a value $\kappa^2 = 0.01$, a very different behavior is observed. The smaller soliton is also oscillating instead of exit-

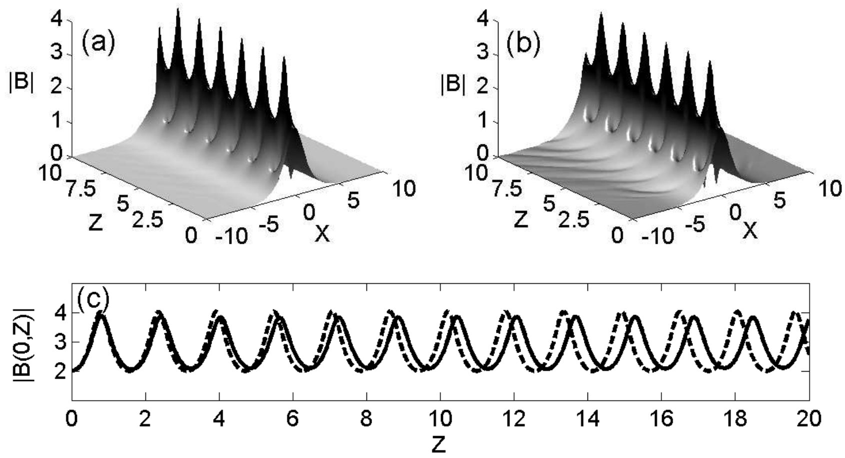

Figure 7: Propagation of a paraxial two-soliton bound state in uniform medium (a) using the NLS equation (denoted by $\kappa^2 = 0$) and (b) using the NNLS equation with $\kappa^2 = 0.01$. Notice that the paraxial case describes the periodic breathing without any radiation while the nonparaxial approach accounts for the radiated field. In (c) we plot the on-axis amplitude obtained from the NLS equation (dashed) and the NNLS equation (solid). It is clearly seen that the nonparaxial propagation has a smaller peak amplitude and a longer period of the focusing-defocusing cycle compared to the paraxial case.

ing from the waveguide. Since the oscillation period of these solitons are different, they show consecutive collisions during propagation.

Further essentially different behavior of paraxial and nonparaxial models can be observed when we take $\eta_0 = 1$, see Figure 9. As in the case of $\eta = 0.75$, the paraxial two-soliton bound breaks up into two solitons of different amplitudes. In this case, after break up, the smaller soliton also exits from the waveguide whereas the higher one oscillates inside the waveguide. When we implement the NNLS equation with $\kappa^2 = 0.001$, a different behavior is observed. The two solitons resulting from the break up remain oscillating in the waveguide and collide with each other. When the degree of nonparaxiality is increased to $\kappa^2 = 0.01$ the nonparaxial model produces another different phenomenon. Here, the higher amplitude soliton has a much bigger transversal acceleration such that the bound state "breaks up" before it swings. After the break up, the two solitons show parallel oscillations but with different periods and trajectories which cause a consecutive collision.

In Figure 8 and 9, we also observe that in the regions where the beam envelope is changing rapidly, e.g. in the area of the splitting process or in the region of collisions, the beam is radiating. The bigger the amplitude (η_0) and the degree of the nonparaxiality lead to larger radiation, see Figure 8.(c) and Figure 9.(c).

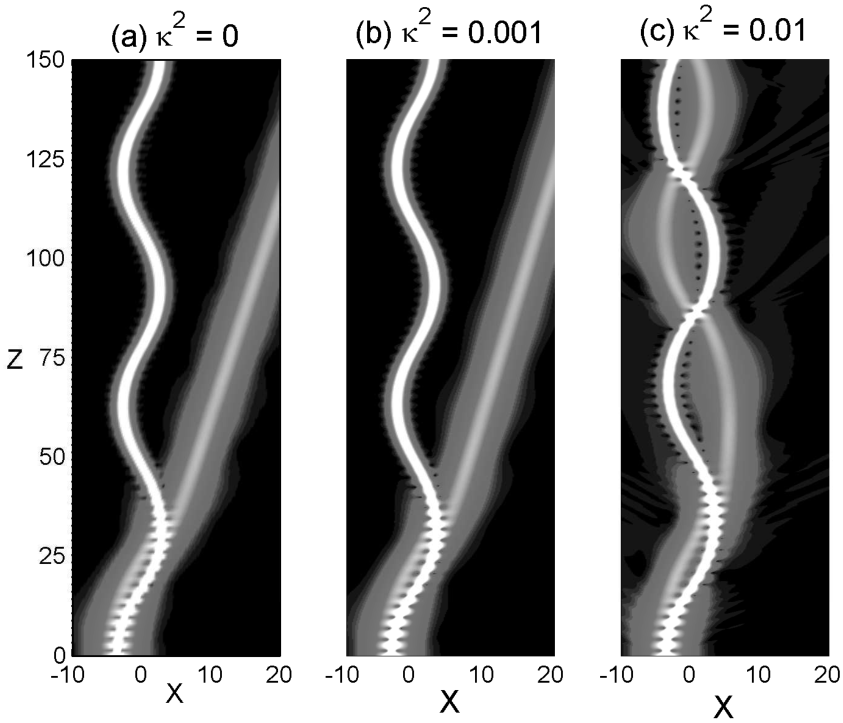

Figure 8: Break up of the paraxial bound-2-soliton with $\eta_0 = 0.75$ in a Gaussian waveguide for $\kappa^2 = 0, 0.001$ and 0.01.

7 Concluding remarks

We have extended the NLS equation to the NNLS equation by including the higher order terms of the NLH equation to study the propagation of weakly nonparaxial (1+1)D beams in inhomogeneous Kerr media. The NNLS equation is still a unidirectional wave equation which means that all back-reflections are neglected. However, it is shown that the accuracy of the NNLS equation is beyond that of the NLS equation. Based on the NNLS equation we found analytically and numerically that when a stationary nonparaxial soliton is placed in a Gaussian waveguide, it oscillates inside the waveguide where a higher amplitude soliton has a larger oscillation period. This behavior is similar to the case of the paraxial soliton. The difference is that the nonparaxial soliton has a longer oscillation period compared to that of the paraxial soliton of the same amplitude. A larger degree of nonparaxiality leads to a longer oscillation period. Based on this propagation property we study numerically the break up of a multisoliton bound state in a Gaussian waveguide. Since the break up process of a multisoliton bound state depends very much on the oscillation period of each soliton contained in the bound state, the behavior of the bound state break up produced by the NNLS equation may be very different from that predicted by the paraxial equation.

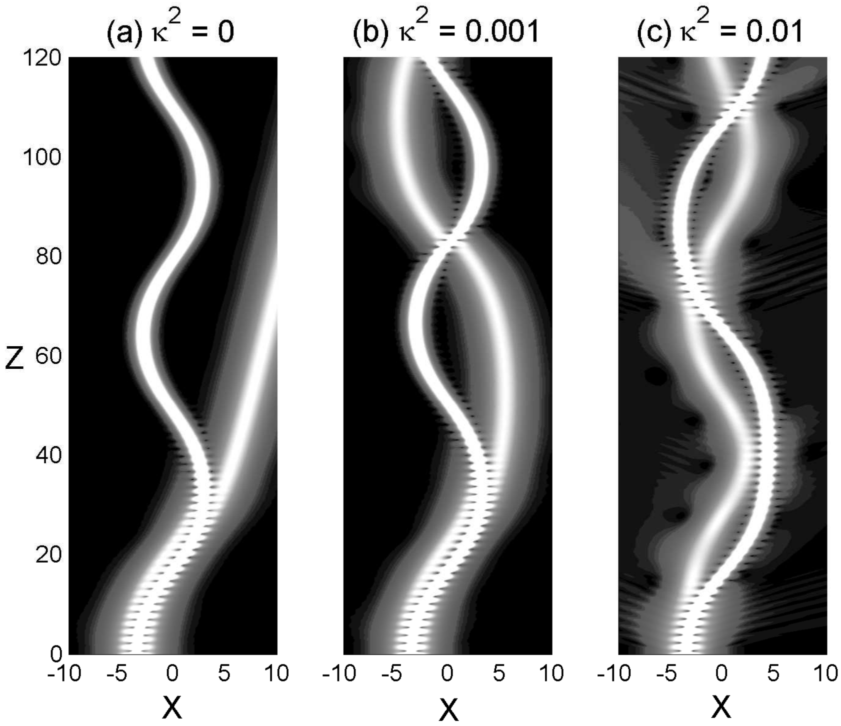

Figure 9: Same as for Figure 8, but for $\eta_0 = 1$.

Acknowledgment

We would like to thank H.J.W.M. Hoekstra (University of Twente, Netherlands) and Andonowati (Institut Teknologi Bandung, Indonesia) for the stimulating discussions and the facilities provided for this research. This research was partly conducted at KPP-MIT, Modeling and Simulation Col-laboratory, Institut Teknologi Bandung, Indonesia. Partial financial support from KNAW-Scientific Programme Indonesia-Netherlands (Mobility Programme 03-MP-15); and from the Technology Foundation STW (TWI. 4813), Applied Science Division of NWO and the technology programme of the Ministry of Economic Affairs, The Netherlands are gratefully appreciated.

References

[1] Y.S. Kivshar and G.P. Agrawal, *Optical solitons: From fibers to photonic crystal*, (Academic Press, San Diego, 2003).

[2] S. Trillo and W. Torruellas, *Spatial Solitons*, (Springer-Verlag Berlin Heidelberg, Germany, 2001).

[3] V.E. Zakharov and A.B. Shabat, Exact theory of two-dimensional self-focusing and one-dimensional self-modulation of waves in nonlinear media, *Sov. Phys. JETP,* **34**, 62 1972.

[4] N.N. Akhmediev and A. Ankiewicz, *Solitons: Nonlinear pulses and beams*, (Chapman & Hall, London, 1997).

[5] A. Suryanto, E. van Groesen and H.J.W.M. Hoekstra, Deformation of modulated wave groups in third order nonlinear media, *Opt. Quant. Electron.* **33**, 513, 2001.

[6] A. Suryanto and E. van Groesen, On the swing effect of spatial inhomogeneous NLS solitons, *J. Nonlin. Opt. Phys. Mat.* **10**, 143, 2001.

[7] A. Suryanto and E. van Groesen, Break up of bound-N-spatial-soliton in a ramp waveguide, *Opt. Quant. Electron.* **34**, 597, 2002.

[8] A. Suryanto and E. van Groesen, Self-splitting of multisoliton bound states in planar Kerr waveguides, *in preparation*, 2004.

[9] P. L. Kelley, Self-focusing of optical beams, *Phys. Rev. Lett.* **15**, p. 1005, 1965.

[10] E.L. Dawes and J.H. Marburger, Computer studies in self-focusing, *Phys. Rev.* **179**, p. 862, 1969.

[11] M. Karlsson, Optical beams in saturable self-focusing media, *Phys. Rev.* **A46**, p. 2726, 1992.

[12] E. Yablonovitch and N. Bloembergen, Avalanche Ionization and the Limiting Diameter of Filaments Induced by Light Pulses in Transparent Media, *Phys. Rev. Lett.* **29**, p. 907, 1972.

[13] Kh.I. Pushkarov, D.I. Pushkarov and I.V. Tomov, Self-action of light beams in nonlinear media: soliton solution, *Opt. Quant. Electr.*, **11**, p. 471, 1979.

[14] M.D. Feit and J.A. Fleck, Beam nonparaxiality, filament formation, and beam breakup in the self-focusing of optical beams, *J. Opt. Soc. Am.* **B5**, p. 633, 1988.

[15] N. Akhmediev, A. Ankiewicz and J.M. Soto-Crespo, Does the nonlinear Schroedinger equation correctly describe beam propagation?, *Opt. Lett.* **18**, p. 411, 1993.

[16] J.M. Soto-Crespo and N. Akhmediev, Description of the self-focusing and collapse effects by a modified nonlinear Schrödinger equation, *Opt. Commun.* **101**, p. 223, 1993.

[17] A.P. Sheppard and M. Haelterman, Nonparaxiality stabilizes three-dimensional soliton beams in Kerr media, *Opt. Lett.* **23**, p. 1820, 1998.

[18] G. Fibich, Small Beam Nonparaxiality Arrests Self-Focusing of Optical Beams, *Phys. Rev. Lett.* **76**, p. 4356, 1996.

[19] Q.S. Chang, E.H. Jia and W. Sun, Difference schemes for solving the generalized nonlinear Schrödinger equation, *J. Comput. Phys.* **148**, p. 397, 1999.

[20] G.R. Hadley, Transparent boundary-condition for beam propagation, *Opt. Lett.* **16**, p. 624, 1991.

[21] J. Satsuma and N. Yajima, Initial Value Problems of One-dimensional Self-Modulation of Nonlinear Waves in Dispersive Media, *Suppl. Prog. Theor. Phys.* **55**, 284, 1974.

[22] A. Hasegawa and Y. Kodama, *Solitons in optical communications*, (Clarendon Press, Oxford, 1995).

[23] F. Garzia, C. Sibilia, M. Bertolotti, Swing effect of spatial soliton, *Opt. Commun.* **139**, 193, 1997.